Research Article   **Open Access**

Fibroblast Cell Cultivation on Wooden Pulp Cellulose Hydrogels for Cytocompatibility Scaffold Method

Takaomi Kobayashi1* and Karla L Tovar-Carrillo2

[1]Department of Materials Science and Technology, Nagaoka University of Technology, 1603-1 Kamitomioka, Nagaoka, Niigata 940-2188, Japan
[2]Biomedical Science Institute, Universidad Autonoma de Cd. Juarez, Estocolmo y anillo envolvente del PRONAF, C.P 32315, México

Abstract

Fibroblast cell cultivation method was evaluated by using natural polymers sourced from pulp cellulose in their hydrogel forms. The pulp sourced was offered as an alternative for the preparation of hydrogel films when the cellulose was dissolved in dimethylacetamide/lithium choride (DMAc/LiCl) solution and converted hydrogels having flexible and transparent properties. The cultivation of the fibroblast cells was investigated on the hydrogels obtained in different LiCl concentration in the range of 4 to 12 wt%. Regarding the cytocompatibility, when NIH 3T3 fibroblast cells were used for cell adhesion assays, the growing cells showed higher density and aspect ratio on the hydrogel films than the observed on the commercial polystyrene dish (PS dish) used for cell cultivation. The mechanical and surface tests showed that the hydrogel films had elongation around 20 and 40 %, tensile strength from 48 to 67 N/mm^2, and high water content value from 200 to 320 %. The results showed that cell addition and spreading on the hydrogel was higher compared with that in the PS dish used as control. Moreover, according with cell morphology tests, the values of cell area, long axis, and aspect ratio were higher than the registered on PS dish. These exhibited that the cellulose hydrogel films prepared with wooden pulp provided good cytocompatibility for its application in tissue engineering.

Keywords: Fibroblast; Cytocompatibility; Cellulose; Hydrogel; Pulp

Introduction

In recent years, artificial materials are of growing importance in medicine and biology. A modern scientific interdisciplinary field known as tissue regeneration has been developed to design artificial biocompatible materials to substitute damaged tissues and organs. The adhesion of cells to a substratum is a prerequisite for the survival and proliferation of most normal eukaryotic cells. The role of the extracellular environment is vital in determining cellular behavior. Modification of surface topography has been shown to produce changes in differentiation, immunosuppressive properties, adhesion, and proliferation, when compared with cells cultured on unmodified substrates [1-4]. Conventional cell culture systems, such as tissue culture polystyrene (PS dish), lack significant, physical surface topography, and often generate cells that do not model their native tissue. Therefore, it is a necessity for culture scaffolds and matrices to mimic a native environment and provide a physiologically relevant system for investigating cells in vitro. Research in developing textured or porous culture scaffolds is being carried out, but how surface morphology affects cells adhesion and proliferation is still poorly understand. Fields that require control of cell function and guidance, such as tissue engineering, and implantable biomaterials, need a low cost and simple scaffold fabrication method for a culture platform. The platform should provide an environment where extracellular (ECM) and signaling can be driven by surface topography and customized to mimic an in vivo system [2-6]. Hydrogels have been the primarily choice for a large number of researchers for many applications in regenerative medicine due to their unique biocompatibility as scaffolds [2-7]. The functional obligation of the tissue scaffold is to maintain cellular proliferation. Therefore, finding a critical design for hydrogel in regenerative medicine is considered still in the transition on the healing process [8-12]. In addition, functionality in the scaffold and the emergent tissue during scaffold biodegradation is still remaining as a future development in research. So far, both natural and synthesized polymers have been used as supporting matrix for tissue repair and regeneration [8-11]. Natural polymers showed advantages over

synthetic polymers to maintain cellular proliferation. Polymers of natural origin offer attractive options, mainly due to their similarities with ECM as well as chemical versatility and biological performance. It is well known that the widely considered natural polymers include collagen, chitosan, chitin, starch, and cellulose and their excellent biocompatibility and safety is a result of their biological characteristics [12-18]. Furthermore, cellulose is regarded as the most common biopolymer in nature and one of the useful and sustainable biopolymer [19-25].

The excellent biocompatibility and safety of cellulose make this biopolymer an important source in modern medical applications. In general, biodegradable biomaterials are desirable in tissue engineering to be replaced by newly formed tissue upon regeneration. In the case of wound dressing, when the wound closes or fully heals, then the material falls off. For example, hydrogels provide a moist wound covering conductive to healing, and also protect the wound from infection. A disadvantage of many hydrogel networks, however, is their lack of strong mechanical properties [25,26]. The excellent biocompatibility and safety of cellulose make it an important source in modern medical applications as the case of wound dressing, in which a material to maintain a moist environment at the wound interface, acting as a barrier to microorganisms and remove excess exudates and promote wound healing is needed [20,25,26]. Several approaches have been done

to elaborate cellulose hydrogels films using cross linkers or modifying cellulose structure to improve its solubility. Since even fewer are known to deal with effective applications of cellulose for hydrogel materials [27,28], most of the academic works have been reported preparation of biomaterials using cellulose derivatives or cellulose powder but none using cellulose fibers from waste product for biomedical applications. We report firstly here cellulose hydrogel films showing very good mechanical properties and bio and cytocompatibilities.

In our previous work, we elaborate cellulose hydrogels using agave bagasse as cellulose source. The obtained hydrogel films showed good cyto-biocompatible properties for medical applications [29]. The aim of this study was to offer an alternative use of industrial waste products reach in natural polymers to elaborate materials for medical applications.

In the following article, we used pulp fibers, another industrial waste product, to elaborate hydrogel films, even though several approaches have been made previously in order to elaborate films using cellulose fibers. Until the present day, no research has been conducted to study such cellulose hydrogels. Therefore, this work focuses in the fibroblast cultivation on pulp hydrogels films method and properties of cyto- and bio-compatibility and mechanicals on the cellulose films. When the hydrogel films were prepared by phase inversion, it was found that these properties depended upon LiCl content in the dimethylacetamide (DMAc) solution. Thus, evidence on broad in vitro cyto and biocompatibility presented that the hydrogels are very useful for medical applications, especially in tissue engineering.

Experimental Methods

Materials

Pulp cellulose fibers were provided from Hokuetsu Kishu Paper Mill CO. (Japan). As a solvent, N, N, dimethylacetamide (DMAc) was purchased from TCI (Tokyo, Japan) and stored for more than 5 days with potassium hydroxide before uses. Lithium chloride (LiCl) was dried at 120°C for 12 h in a vacuum oven. Ethanol was purchased from Nacalai Tesque. Inc (Tokyo, Japan). For protein adsorption studies, bicinchoninic acid (BCA) kit was purchased from Sigma Aldrich (Tokyo, Japan). Fetal bovine serum (FBS, Cell Culture Bioscience), bovine serum albumin (BSA, Sigma Aldrich), phosphate-buffered saline (PBS, Dullbecco Co., Ltd.) were used. Trypsin-0.053 M-ethylenediaminetetraacetate (trypsin-EDTA) was purchased from Gibco (Tokyo, Japan) and formaldehyde (37 vol% aqueous solution) was from Wako Co., Ltd. NIH 3T3 mouse embryonic fibroblast cells were also purchased from BioResource Center (Japan).

Preparation of hydrogel films

The pulp cellulose solutions in DMAc-LiCl system were prepared by following with modification of report [30-37] at different LiCl concentration from 4 to 12 wt%. The pulp cellulose fibers were firstly treated with water, ethanol, and finally DMAc by stepwise solvent exchange processes. The pulp cellulose fibers (1 wt%) were suspended in 300 mL of distilled water and left overnight to allow swelling of the fibers. Then, water was removed by an adapter glass filter under vacuum. On following process, ethanol (300 mL) was added to the swelled fibers and the mixture was stirred for 24 h with 2 rpm. After ethanol was removed by filtration, the pulp fibers were added in 300 mL of DMAc solution, which also was included a LiCl content ranging from 4 to 12 wt% of concentration. Finally, the solution was left overnight under stirring condition. As a result, transparent pulp solutions were successfully obtained. The preparation of the cellulose hydrogel films

by phase inversion of the transparent solution to gelatinous solid was carried out as followed. A weighed amount of the cellulose solution was poured into a glass tray (10 cm diameter) and kept for 12 h in a container filled with 30 mL of ethanol as coagulant. The resulting films were wasted by ethanol 3 times and then, the cellulose films were submerged in 100 ml of distilled water and placed in shaking bath at 25°C to remove remain DMAc, distilled water was changed each 2 h. Pulp hydrogel films were kept in shaking bath for 12 h. Finally, the hydrogel films were immersed in distilled water over night and kept in phosphate buffered saline (PBS) at 4°C in a plastic container. This procedure was repeated 3 times.

Cytotoxicity of hydrogel films

Hydrogel films circles with 30 mm diameter were used for cell seeding purposes. The samples were sterilized with 70 and 50 wt% of aqueous ethanol twice for 30 min and then, rinsed twice with PBS for 30 min. Finally, the hydrogel samples were swelled in DMEM for 2 h before starting the seeding procedure. The NIH 3T3 mouse embryonic fibroblast cells were cultured at 37°C in 95 wt% of relative humidity and 5 wt% of CO_2 environment. The culture medium was in 90 wt% of DMEM supplemented with 10 wt% FBS and 1 wt% penicillin/streptomycin. The cells were seeded on the hydrogel films and on tissue culture polystyrene dish (PS dish) with 35 x 10 mm size (used as control), with cell density of 8 x 10^3 cm^{-2}. The cells were used for imaging and characterization purposes after 3, 7 and 14 days of culture. The sample image was obtained using an inverse microscope (Olympus CKX41, Japan) and was then analyzed for cell elongation and directionality using cellsens digital imaging software. To measure cell area, the cell boundaries were marked by the PC operation. Also aspect ratio, long axis and cell density were measured from by image data. Approximately, 50 cells were analyzed per image. For each sample, five images were analyzed to obtain an unbiased estimation of the cell morphology. The results presented herein were based on three independent experimental runs.

In vitro biocompatibility experiments

In the case of protein adsorption, quantitative single protein adsorption experiments in PBS were determined by bicinchoninic acid assay [29,35]. Bovine serum albumin (BSA) and fetal bovine serum (FBS) were used. Protein concentration of serum proteins was 1 mg/mL Hydrogel disks, 5 mm in diameter, were equilibrated in PBS for a period of 24 h and then immerged in 1 mL of PBS containing known serum proteins for 4 h at 37°C. Following the adsorption experiments, the hydrogel disks were rinsed 3 times then transferred into a plastic tube containing 5 mL of 2 wt% aqueous solution of sodium dodecyl sulfate (SDS) and shaken for 4 h at room temperature to elute the proteins adsorbed to the hydrogels. During screening experiments, we determine that an elution time of 4 h removed all adsorbed proteins. The amount of adsorbed proteins was calculated from the concentration of proteins in the SDS solution read at 562 nm and calibration curve prepared from pure sample was used. Four repeats (3 disks per repeat) were measured and the average value was taken.

Clotting experiments were performed in a microplate reader instrument Multiskan Go (Thermo Scientific) [29,35]. The instrument could maintain a chosen temperature during the experiment period. Samples were shaken only once, for 20 s (low speed just before the first reading). Hydrogel disks 5 mm in diameter were cut from casted films. Temperature 37°C was set and readings were repeated every 30 s. Readings were performed with a 545 nm filter and were recorded in a computer memory for further evaluation. 100 μL of platelet poor

plasma (PPP) was mixed with 100 μL of PBS and 100 μL of water in a 96 well flat-bottom microplate. The sample surfaces in a microplate have to be free from air-bubbles in order to get well reproducible curves. Controls for 100% PPP and PBS were observed during the whole period of measurements. Immediately before the reading, calcium chloride (50 μL) was added. The clotting agents were injected to the exanimated samples with a multichannel pipette. The collected data were finally evaluated using a computer program.

Platelet adhesion experiments were conducted using hydrogel disks (5 mm in diameter) equilibrated with PBS overnight. A total of 0.6 mL of PRP was transferred to 24-well culture plates, and the PBS equilibrated hydrogels were placed into the PRP containing wells. Incubation was carried out at 37°C for 2 h, and then the hydrogel disks were removed and rinsed with 1 mL of PBS to remove loosely attached platelets. Platelet counting was estimated by photometric method using plastic cuvettes, with 10 mm optical path. The measurements were performed at $\lambda=800$ nm. The formula for platelet count calculation is as follows:

$$N\ (10^8/mL) = (6.23/2.016\text{-}k*\lambda*E/800 - 3.09) * R$$

Where N is the estimated platelet count per milliliter, R is the examined sample dilution, λ is the used wavelength, E is the measured extinction of the sample and k is a geometrical factor equal 1 for 10 mm optical path. The equation was tested and is correct for measurements performed for λ ranged from 600 to 800 nm. PRP was diluted ten times for each measurement and the instrument was set for zero with the reference sample-plasma or buffer, both free from platelets. On following this, the hydrogel films were rinsed for three times with PBS (37°C) and the adhered platelet were fixed with 1 ml of 2.5 wt% glutaraldehyde/PBS at 4°C for 2 h. Finally, the hydrogel films were immersed into the PBS for 5 min and dehydrated twice as followed. The first dehydration was carried out with a series of ethanol/PBS mixtures with increasing ethanol concentrations (25, 50, 75, and 100 wt%) for 15 min in each mixture. The second dehydration was performed with of iso-amyl acetate/PBS mixtures with increasing iso-amyl acetate concentrations (25, 50, and 100 wt%) for 15 min. After freeze-drying the treated samples, the platelet-attached films were coated with a gold layer for the SEM measurements.

Evaluation of hydrogel films

Before the phase inversion process, shear viscosity of the cellulose DMAc solutions containing different LiCl concentration was measured by a B type viscometer at 25°C. Water contents of the resultant hydrogel films were determined by weighing the wet and dry samples by following procedure. Samples of 5 mm diameter disks were cut from cast films, dried in a vacuum oven, and weighed. The samples were then swollen in phosphate buffered saline (PBS) for 36 h and blotted lightly with filter paper to remove excess water. The weight of the hydrated samples was then determined. The percent EWC of hydrogels was calculated based on EWC= $W_h - W_d / W_h$ x 100. Where W_h is the weight of the hydrated samples and W_d is the dry weight of the sample. For each specimen, four independent measurements were determined and averaged [38].

Tensile strength and elongation on dry hydrogel films were measured on a LTS -500N - S20 (Minebea, Japan) with universal testing machine equipped with a 2.5 kN cell. Strips with a length of 50 mm and a width of 10 mm were cut from cast film with a razor blade. Strain was recorded by means of Zwick Makrosense clip-on displacement sensors. One set of samples (five strips each) was measured and each set was repeated 3 times. Only samples which ruptured near mid-specimen

length were considered for the calculation of tensile strength. The values of the tensile strength and elongation were calculated by using the following equations:

Tensile strength (N/mm²) = Maximum Load / cross section area

Elongation (%) = ((Final length (mm) – Initial length (mm)) / (Initial length (mm)) x 100

Viscoelasticity of the hydrogel films with 2 cm in diameter and having 5 mm of thickness was determined by Auto Paar- Reoplus equipment (Anton Paar Japan, Tokyo) in wet conditions at 37°C.

FT-IR spectroscopy was applied to examine component in wet hydrogel samples by using a FT-IR 4100 series (Jasco Corp), Japan. The thin hydrogel film was set up in a CaF_2 window (30 mm diameter; thickness 2 mm, Pier Optics Co. Ltd.). Then, 2 μL of distilled water was dropped to the film. Then, another window was pressed to cover the wet film. For measurement of scanning electronic microscope (SEM), after the hydrogel film sample was dried, samples were coated with a gold layer. The SEM images were recorded using JSM-5310LVB (JEOL, Japan) with a magnification of 5000 in magnitude.

Statistical analysis

For continuous variable data, means and standard errors of the mean were computed and, when appropriated, comparisons between two groups were made with unpaired Student's t-test with statistical significance set at $p<0.05$ according to reference [12]. Analyses of multiple groups were made by ANOVA followed by a post-comparison Scheffe test with statistical significance set at $p<0.05$.

Results
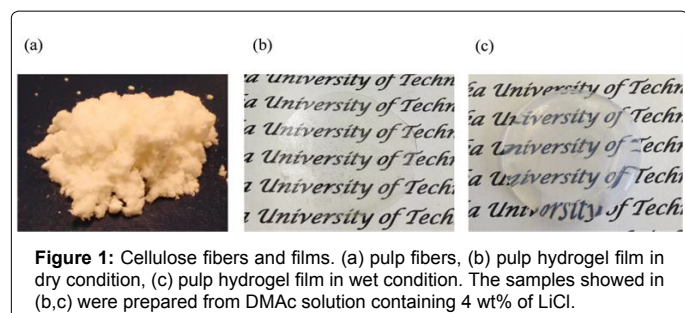
Preparation of hydrogel films

Cellulose hydrogels were prepared changing the LiCl ration from 4 to 12 wt%. Inverse phase coagulation with ethanol was used to prepare the hydrogel films (Figure 1). No significant changes in color were observed in the hydrogel obtained with different LiCl ratio.

Cell density on hydrogel films

The adhesion of NIH3T3 was measured after various times on cellulose hydrogels and PS dish. In order to observe cell adhesion on the hydrogel films, phase-contrast light microscope images were used. Cell morphology of adherent fibroblast on pulp hydrogels was analyzed to determine the effect of LiCl content on cell adhesion and morphology. It was observed that NIH3T3 cells adhered and proliferated well on all surfaces. The cell density on the hydrogel films were evaluated by counting adhered fibroblast on the hydrogel surface. Figure 2 shows cell density of NIH3T3 for pulp cellulose hydrogels. In all cases, the obtained results showed that cell densities in the hydrogel films were higher than the observed on PS dish used as control surface. Attachment of cells occurred on all hydrogel samples (with 4 to 12 wt% of LiCl), and it was observed in the first 30 min. In order to facilitate comparisons of the morphology of the spread cells, incubations were carried out for 4, 12, 24 and 72 h. With the increment of culture time cell density gradually increase. After 72 h passed, the amounts of the cell density in the 4 wt% LiCl were actually higher. In addition, fibroblast was found to have a maximum adhesion on the surface of hydrophilic and soft films [29,38].

Cell mosrphology on hydrogel films

In addition, cell morphology results showed that cell area, aspect ratio, and the length of the long axis were sensitive to LiCl content, as

Figure 1: Cellulose fibers and films. (a) pulp fibers, (b) pulp hydrogel film in dry condition, (c) pulp hydrogel film in wet condition. The samples showed in (b,c) were prepared from DMAc solution containing 4 wt% of LiCl.

shown in Figure 3. In particular, all three parameters showed higher results in smooth surfaces, these differences were significant (ANOVA, $p<0.05$). Projected cell area (j), aspect ratio (k), and length of the long axis (l) decreased systematically with the increment of LiCl content. This was significant in all the hydrogel samples (Student's t-test, $p<0.05$, n=6). An increased in cell area was observed as LiCl concentration increased. This increase was significant for PS dish and LiCl l2 wt% (Student's t-test, $p<0.05$, n=6), and for LiCl 6 wt% (Student's t-test, $p<0.05$, n=6). As shown in Figure 3, results of cell morphology on the hydrogels films revealed a remarkable difference on fibroblast pattern in the morphology for the hydrogel films and commercial PS dish (a-c), these difference were significant (ANOVA, $p<0.05$). After 48 h of cultivation cell area, aspect radio and long axis showed differences compared with PS dish used as control. This was significant in all the hydrogel samples (Student's t-test, $p<0.05$, n=6). An increased in cell area was observed as LiCl concentration increased. This increase was significant for PS dish and LiCl 12 wt% (Student's t-test, $p<0.05$, n=6), and for LiCl 12 wt% (Student's t-test, $p<0.05$, n=6). For example, in the hydrogel film for the 4 wt% LiCl (d-f), the fibroblast surely adhered and grew on the hydrogel film, as observed in the images. After 4 hours of cell culture, the image (b) showed longer axis shape of the grown cells as compared with those adhered on the PS Dish at the same condition. Moreover, the remarkable differences on aspect ratio results were observed when LiCl concentration increased. These differences were significant comparing LiCl 12 wt% and LiCl 6 wt% (Student's t-test, $p<0.05$, n=6). These results confirmed the expected differences of long axis with the increment of LiCl. These differences were significant with PS dish compared with LiCl 4% and LiCl 12 vol% (Student's t-test, $p<0.05$, n=6).

The morphology of cells spread on cellulose hydrogels was similar in all the LiCl contents, except that there was an increase in the in cell area, aspect ratio, and length of the long axis depending of the LiCl content. In the case of PS dish, cells spread had different morphologies. The cell bodies were generally rounded. Cells spreads on cellulose hydrogels showed large filipodial extensions. These extensions generally penetrated into the hydrogel matrix, whereas the cell bodies stayed on top. Sometimes, however, the entire cell penetrated into the matrix. In order to observe the adhesion pattern of the cells on the hydrogel matrix, fluorescence dyeing was carried out. Figure 4a and 4b shows fluorescence dyeing of attached cells on hydrogel films with 6 wt% and 12 wt% of LiCl, respectively.

Evaluation of biocompatibility of hydrogel films

Protein adsorption of BSA and FBS was evaluated for biocompatibility tests. It is well known that protein adsorption is directly affected by materials surface characteristics and plays an important role on cell adhesion and spreading. Therefore, it is interesting in the present work to study protein adsorption on the hydrogel films for BSA

and FBS serum proteins. Figure 5 shows adsorption of BSA and FBS examined in vitro for each hydrogel film. As prepared by different LiCl content in the DMAc solution, the amounts of BSA on the hydrogels films increased with the increase of the LiCl contents. Furthermore, blood compatibility of the hydrogel films was studied as shown in Figure 5a. Herein, after the hydrogel samples were in contact with platelet poor plasma (PPP), the time of cloth formation was measured. The results demostrated that the time of the cloth formation was affected by the LiCl contents in the DMAc solution.

Evaluation of hydrogel films

Evaluation of the properties of pulp cellulose hydrogels was made. Table 1 shows the obtained results for water content (%), elongation (mm), tensile strength (N/mm²) and shear viscosity of the DMAc solutions containing different contents of LiCl. As it can be observed on Table 1, remarkable differences were observed in the obtained results of hydrogels elaborated with different content of LiCl.
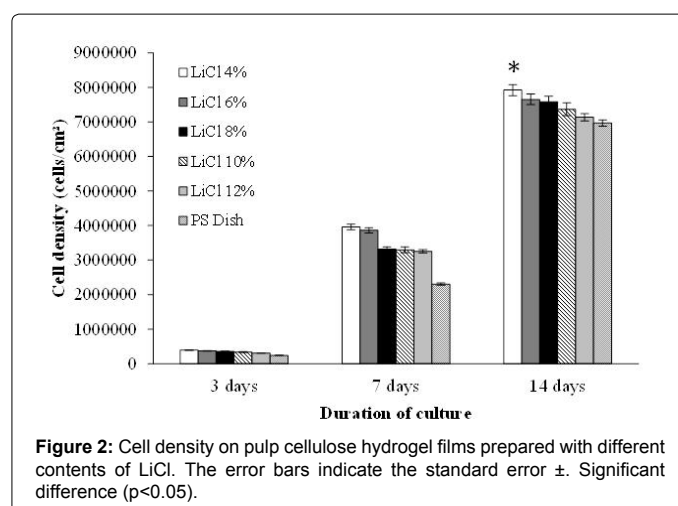
Discussion

Preparation of hydrogel films

Figure 1 shows pictures of (a) Pulp cellulose fibers, (b) Transparent dry hydrogel, and (c) the wet film. Moreover, no difference in color or appearance was observed between pulp hydrogels and the obtained in our previous work. In order to prepare hydrogel films of the pulp fibers (a), the fibers were dissolved in DMAc solution having 4-12 wt% of LiCl after solvent exchange between water, ethanol, and DMAc. Shear viscosity of the obtained transparent DMAc solution of pulp cellulose was measured, when the LiCl content was changed.

Cell density on hydrogel films

For the cell adhesion measurements, several times on cellulose hydrogels and PS dish were used. Cell morphology of adherent fibroblast on pulp hydrogels was analyzed to determine the effect of LiCl on cell adhesion and spreading. According with the results obtained by Grinnell et al. [16], fibroblast preferred soft surface for proliferation. In the present work, the difference in the cell density between the hydrogels prepared with 4 wt% and 12 wt% of LiCl seemed to be related to the samples softness depending of the concentration of LiCl used to prepare the film. In the case of lower content of LiCl, the
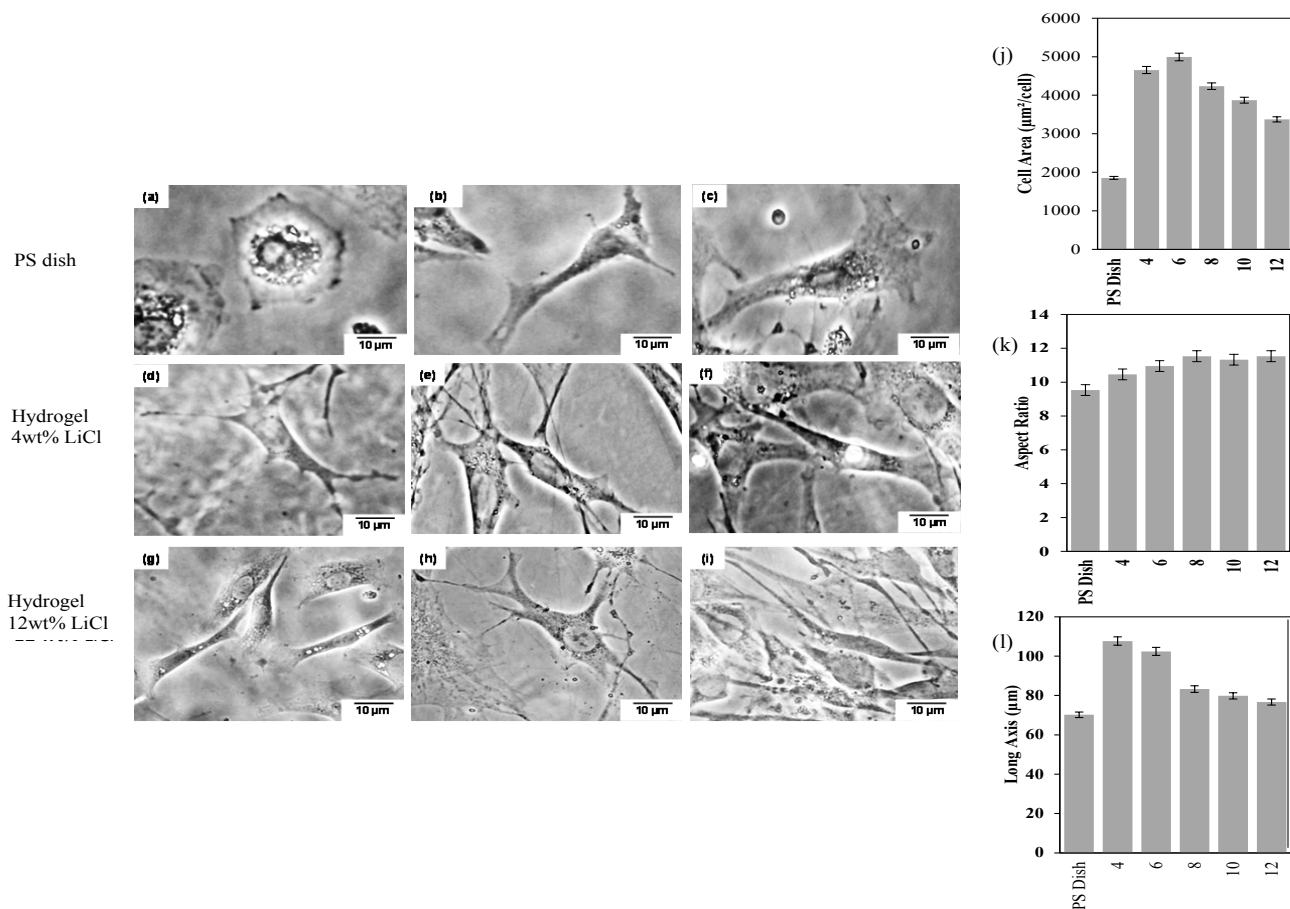

Figure 2: Cell density on pulp cellulose hydrogel films prepared with different contents of LiCl. The error bars indicate the standard error ±. Significant difference ($p<0.05$).

Figure 3: Phase-contrast light images of (a-f) hydrogel films and (g-i) commercial PS dish. (a-c) hydrogel films prepared with 4 wt% of LiCl, (d-f) 12 wt% of LiCl. The cell culture time was (a,d,g) 4 h, (b,e,h) 24h and (c,f,i) 48 h. Effect of the LiCl content on (j) projected area, (k) aspect ratio, and (l) length of long axis at cell culture time of 48 h. PS dish was used as control. Bars correspond to the mean ± standard deviation for n= 110 for hydrogel surfaces prepared with different concentration of LiCl.
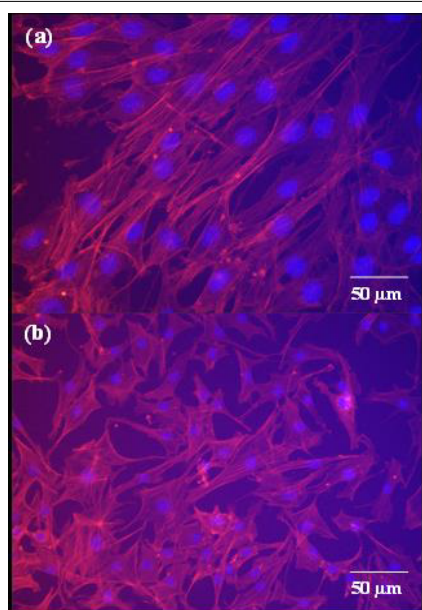

Figure 4: Fluorescence dyeing of adhered cells on hydrogel films prepared with different LiCl content after 4 h of cell culture. Adhered cell on hydrogel with 6 wt% of LiCl (a), adhered cells on hydrogel with 12 wt% LiCl (b).
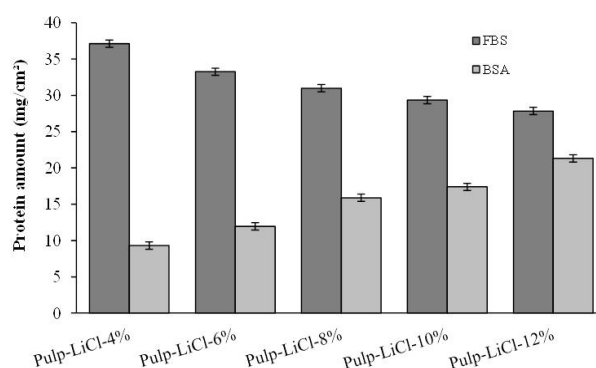

Figure 5: Protein adhesion of hydrogel films prepared from DMAc solution containing different LiCl concentration. The error bars indicate the standard error ±.

softness and stiffness of the films might regulate the adhesion between cellular- extracellular matrix molecules. Additionally, cell culture time was extended to 7 and 14 days and after this time no cytotoxic or decreased in cell density was found. Less cell adhesion values in the first 3 days were observed in pulp films comparing to the reported in agave films. This could be attributed to the difference in the mechanical properties of the hydrogels films affecting the surface resulting in a decrease of the number of adhered cells.

Samples	Water content (%)	Elongation (mm)	Tensile Strength (N/mm²)	Shear viscosity (Cp) 6 rpm	60 rpm
Pulp-LiCl-4%	321 ± 0.61	8 ± 0.21	48 ± 0.2	203 ± 1	200 ± 2
Pulp-LiCl-6%	283 ± 0.92	13 ± 0.77	51 ± 0.5	411 ± 3	407 ± 1
Pulp-LiCl-8%	241 ± 0.54	15 ± 0.26	62 ± 0.3	621 ± 2	617 ± 4
Pulp-LiCl-10%	225 ± 0.23	19 ± 0.84	66 ± 0.1	985 ± 4	979 ± 6
Pulp-LiCl-12%	192 ± 0.91	20 ± 0.65	*67 ± 0.3	*1426 ± 2	1422 ± 5

Each column represents the mean (± s.e.m) number of samples tested at 25°C to obtain a relied value. Mean ± s.e.m for n=5 for each test. An asterisk indicates statistical differences from the film prepared with 12 wt% of LiCl ($p < 0.05$).

Table 1: Properties of hydrogel membranes of pulp.

Cell mosrphology on hydrogel films

Diminished projected cell area is consistent with Grinnell et al. [16], who reported smaller projected areas for BHK fibroblast on less smooth surfaces. Two plausible explanations for diminished cell spreading on samples with higher LiCl content are related to the role of focal adhesion complexes in mediating cell adhesion to biomaterials. Focal adhesion contains clusters of integrin transmembrane adhesion receptors that bind the EMC proteins (e.g., fibronectin, collagen) adsorbed to biomaterial surface. Consequently, it is plausible that the change of the roughness on the film surface undermine cell spreading and morphology by limiting the number of integrin receptors engaged in cell adhesion.

Moreover, the boundaries of the adhered cells on cellulose films seemed to be tightly adhered on the hydrogel surface, showing a diffuse shape on the cultivated cell edge. In addition, anisotropic shape was observed in the first hours of the cell culture, when the hydrogel films were used in the scaffold on the cell growing. Relative to the hydrogel film, the fibroblast shape observed on PS dish (a) was mainly round at 4 hours, as the anisotropic shape seen in (g) on the hydrogel with 12 wt% of LiCl. This indicated that the cell seems not to be tightly adhered to the surface of the commercial dish. Comparing with fibroblast shape shown in (d) and (g) for the hydrogels films, these demonstrated a much cytocompatibility to the hydrophilic and soft surface of the hydrogel films. When the LiCl was increased in the DMAc solution to be 12 wt%, the resultant hydrogels films showed lower aspect ratio, long axis and cell density. This might be due to the decreased swelling and softness of the sample film by the formation of macrocation in the film. These results revealed that the hydrogel films made of pulp cellulose provided a better surface for fibroblast growing. Moreover, no significance differences in cell morphology adhered on pulp and agave films were observed.

Due to different cell adhesion patterns were observed depending of LiCl content, fluorescence dyeing was carried out. Fluorescence dyeing shows more detailed cell morphology after the adhesion on cellulose hydrogel surface. Remarkable difference in the spreading pattern was observed when the LiCl content was varied. Figure 4a shows more ordered and aligned cell spreading compared with the non-ordered cell spreading observed on films prepared with 12 wt% of LiCl. On hydrogel with 6 wt% of LiCl, the NIH3T3 cell bodies and microextensions seems to be in close association with cellulose fibers. Cellulose fibers seem to be the method by which the cells were moving into the cellulose lattice. It is significant that differences in cellulose fibers arrangement depending of LiCl were observed, resulting in different cell adhesion patterns as showed in Figures 4a and 4b.

Evaluation of biocompatibility of hydrogel films

It is known that such hydrophilic hydrogel shows to have better tendency for biocompatibility including protein interaction with the scaffold. Such protein adsorption is the first stage of the interactions between the substrate and the body. However, the results observed in the FBS expressed opposite tendency related to those of the BSA. It was known that BSA tended to bind onto hydrophobic surface, meanwhile FBS preferred hydrophilic surface [38,39]. In the present work, the BSA adsorption tended to suppress cell adhesion, as the LiCl concentration was higher. The obtained results showed that FBS adsorption became higher in all cases. In this case, it could be considered that the predominant adsorption of BSA and FBS might be due to hydrogel nature depending upon the LiCl contents. Base on the obtained results with FBS, it would be expected that the hydrogel films prepared with lower LiCl concentration might promoted such cellular adhesion. In addition, more protein adsorption was observed on pulp hydrogels than in agave hydrogels.

As seen, the value of the time of clot formation increased with increasing of the LiCl content used. This phenomenon could be supported with the obtained results of the FBS adsorption as shown in Figure 5. In protein adsorption capacity of the hydrogel films, it was easy to consider that the fibrinogen adsorption might be enhancing to form a fibrin rich cloth. Moreover, the incubated hydrogel disks in PRP were analyzed by SEM. Platelet adhesion results for these pulp hydrogels are shown in Figure 5b and the typical SEM photographs are shown in Figure 6c-6e. Platelet deposition behaviour showed that pulp hydrogels had good blood-contact properties. The number of adhered platelet showed a tendency to decreased with increasing of LiCl content. These results seem to be related to the properties of hydrogel surface investigated by AFM. As shown in Figure 6c-6e, the SEM images revealed that results in platelet adhesion was lightly supressed at lower LiCl content in the DMAc solution. In addition, higher number of platelet was observed on the surface of samples prepared with 12 wt% of LiCl. Similar results were also reported for the adhesion of platelets [39]. They indicated that the hydrogel films could provide a suitable environment to promote and enhance the platelet adhesion regardless to the LiCl used. Moreover, no significance differences were observed in the obtained results conserning clot time and platelet adhesion in pulp and agave films.

Evaluation of hydrogel films

Shear viscosity of the hydrogel films was measured. It was noticed that when the amount of LiCl increased in the solution, both values of shear viscosity measured at 6 and 60 rpm increased. The obtained results at 6 and 60 rpm did not show significant difference, meaning that the pulp cellulose in the DMAc solution had less hydrogen bonding between the cellulose chains. As the viscosity was increased at higher LiCl concentrations, similar phenomena were also presented in references [32,33], indicating that the LiCl added formed a macrocation with cellulose fibers in the DMAc solution. Therefore, in the present work, when the LiCl content increase in the DMAc solution, the interaction cellulose fiber-solvent and interactions fiber-
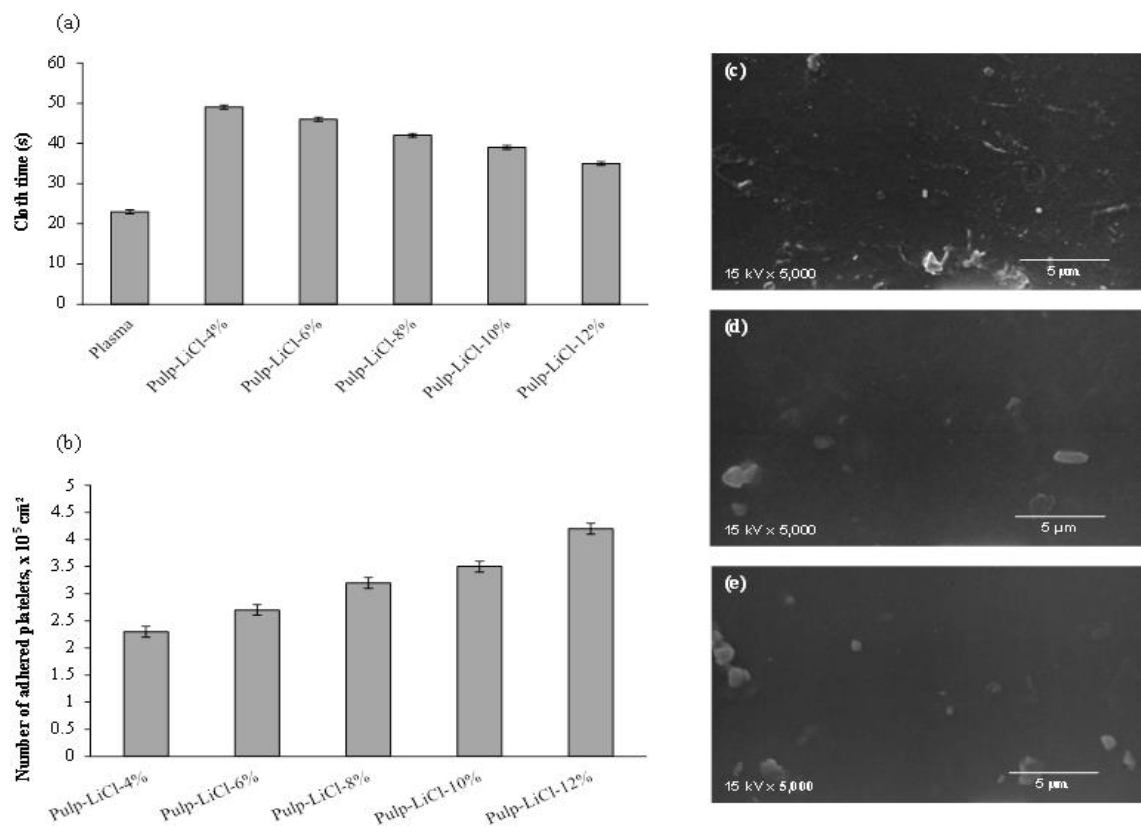
Figure 6: Left side, (a) Clotting time of cellulose hydrogel films prepared with different contents of LiCl, (b) Protein adhesion on cellulose hydrogel films. The error bars indicate the standard error ±. Right side,SEM images of hydrogel films surface treated with platelet. The LiCl content used was (c) 4 wt%, (d) 10 wt%, and (e) 12 wt%.

fiber increased due to the increasing of the macrocation form by the DMAc/LiCl system reaching to a point in which aggregates form. Base on this, it was reasonable to consider that the increased viscosity was caused by the macrocation effect with the LiCl. Moreover, the effect of the macrocation was also observed and reported in the obtained agave films in our previous work [29].

Table 1 also lists hydrogel film properties, as equilibrium water content at room temperature for 72 h. The values of water content decreased from 32.6% to 19.98% with the increment of the LiCl content from 4 to 12 wt%, respectively, in the DMAc solution. The LiCl dependence on the water content of the films might be due to the increment of the amount of the formed macrocation. Therefore, in the microenvironment of the celluloses, it was reasonable for consideration that the diminished water contents of the hydrogel films were due to the effect of LiCl on the cellulose networks. Thus, when the LiCl content was lower, water molecules were capable of penetrating and interacted easily into the hydrogel films because of lower density on the cellulose networks. Therefore, water contents in the film became higher when the LiCl was lower. It was noted that the hydrogel films had very soft and flexible shape even though there was no chemical crosslinking treatment. For uniaxial tensile testing, the sample hydrogels (50 mm x 10 mm) were placed between two clamps and the hydrogel film was then pulled away. Table 1 shows that higher elongations were observed in the films in comparison with 12 wt% of LiCl content relative to that of 4 wt%. As shown in Table 1, the tensile strength and elongation values increead from 48 N/mm² to 67 N/mm² in the cases of 4wt% and 12wt% of the LiCl, respectively. This might be attribuited to the

increase of LiCl in the DMAc solution, which could enhance the interaction between pulp fibers. As reported in research [32], the cellulose could form intermolecular aggregation by interaction through hydrogen bonds in DMAc/LiCl solution and affect the stiffness of the resultant sample films. The effect thus could improve the resistance to the applied force in the higher LiCl case increasing strength of the hydrogel films [32-35]. Pulp hydrogels showed less water content and elongation values comparing with agave films, suggesting more interaction with the macrocation formed in the DMAc/LiCl system. In addition, difference in length and composition between pulp and agave fibers could also affect the mechanical properties of the obtained films, for this, more studies should be conducted to clarify this manner.

In order to evaluate the wet condition of the hydrogel films, FT-IR measurements were carried out. The hydrogel films were dried under vacuum for 24 h at room temperature and then small amount of water droplet was added to be swelled on the CaF_2 window. Figure 7 show FT-IR spectra of their samples prepared from 4 to 12 wt% of LiCl concentration for (a) wet and (b) dry film condition. The FT-IR spectra of the films had strong peaks around 3550 and 3200 cm^{-1} attribuited to -H band stretching. In addition, the peaks around 1150, 1160, 1120, 1059, and 1035 cm^{-1} refered to C-OH, C-O-C, and C-C ring bands, CH_2 and OH groups, respectively [36-39]. It was notice that the intensity of O-H band stretching increased in pulp hydrogel films in wet conditions. This phenomena meant that water bound to the OH group of the pulp fibers in the network. In the water band around 1400 cm^{-1}, in wet condition, the center peak sightly shift, this suggested that water molecules interacted with the pulp cellulose fibers.
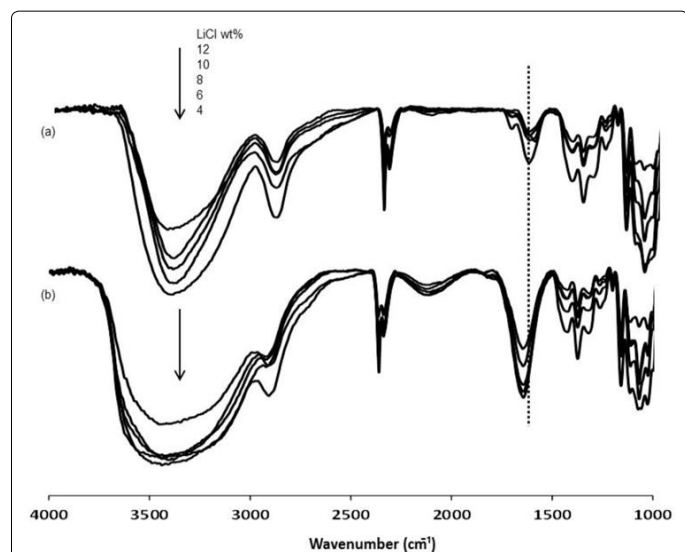
Figure 7: FT-IR spectra of pulp cellulose hydrogel films in (a) dry and (b) wet conditions. LiCl content in the films was varied from 4 to 12 wt%.

Conclusion

Fibroblast adhesion on pulp hydrogels was observed. The content of LiCl in hydrogel films altering fibroblast geometric area and adhesion when compared with fibroblast cultured on PS dish. The results obtained with pulp films were higher than the observed on the commercial dishes used for cell culture. Difference in the mechanical and cyto-biocompatible properties were observed depending of the LiCl content used for the preparation of the hydrogel films. It was proved that the LiCl acted to be dense networks of the cellulose segments and the hydrogel condition influenced in vitro cyto and biocompatibility. These results suggest that these hydrogel films prepared from wooden pulp may have the possibility of usage for biomaterial.

References

1. Stanton MM, Parrillo A, Thomas GM, McGimpsey WG, Wen Q (2015) Fibroblast extracellular matrix and adhesion on microtextured polydimethylsiloxane scaffolds. Journal of Biomedical Materials Research B: Applied Biomaterials 103: 861.

2. Li Y, Huang G, Zhang X, Li B, Chen Y (2013) Magnetic Hydrogels and their potential biomedical applications. Advanced Functional Materials 23: 660.

3. Slaughter BV, Khurshid SS, Fisher OZ, Khademhosseine A, Peppas NA (2009) Hydrogels in regenerative medicine. Advanced Materials 21: 3307.

4. Langer R (1995) Biomaterials and biomedical engineering. Chemical Engineering Science 50: 4109.

5. Uchiyama T, Watanabe J, Ishihara KJ (2002) Biocompatible polymer alloy membrane for implantable artificial pancreas. Membrane Science 208: 39-48.

6. Xu F, Wang Y, Jiang X, Tan H, Li H (2012) Effects of different biomaterials: Comparing the bladder smooth muscle cells on waterborne polyurethane poly-lactic-co-glycolic acid membranes. Kaohsiung J Med Sci 28: 10.

7. Nair LS, Laurenoin CT (2007) Biodegradable polymers as biomaterials. Progress in Polymer Science 32: 762.

8. Sionkowska A (2011) Current research on the blends of natural and synthetic polymers as new biomaterials: Review. Progress in Polymer Science 36: 1254.

9. Silva MR, Castro MCR (2002) New dressings, including tissue engineered living skin. Clin Dermatol 20: 715.

10. Nho YC, Kwon OH (2003) Blood compatibility of AAc, HEMA, and PEGMA-grafted cellulose films. Radiation Physics and Chemistry 66: 299.

11. Henich NA, Kotopodis KP (2002) Clinical characterization of a new polymeric membrane for use in renal replacement therapy. Biomaterials 23: 3853-3858.

12. Barbosa MA, Granja PL, Barrias CC, Amaral IF (2005) Polysaccharides as scaffolds for bone regeneration. ITBM-RBM 26: 212.

13. Castillo-Briceño P, Bihan D, Nilges M, Hamaia S, Meseguer J (2011) A role for specific collagen motifs during wound healing and inflammatory response of fibroblasts in the teleost fish gilthead seabream. Mol Immunol 48: 826.

14. Jayakumar R, Prabaharan M, Sudheesh Kumar PT, Nair SV, Tamura H (2011) Biomaterials base on chitin and chitosan in wound dressing applications. Biotechnol Adv 29: 322.

15. Liu X, Ma L, Mao Z, Gao C (2011) Chitosan-Based biomaterials for tissue repair and regeneration. Advanced Polymer Science 244: 81-127.

16. Grinnell F, Bennett MH (1981) Fibroblast adhesion on collagen substrata in the presence and absence of plasma fibronectin. J Cell Sci 48: 19.

17. Lamprecht FF, Groth T, Albrecht T, Paul D, Gross U (2000) Development of membranes for the cultivation of kidney epithelial cells. Biomaterial 21: 183.

18. Hoenich NA (2004) Update on the biocompatibility of hemodialysis membranes. Hong Kong Journal of Nephrology 6: 74.

19. Muller FA, Muller L, Hofmann I, Greil P, Wenzel MM (2006) Cellulose based scaffold materials for cartilage tissue engineering. Biomaterials 27: 3955-3963.

20. Hoenich N (2006) Cellulose for medical applications: Past, present, and future. Bio resources 2: 270.

21. Sannino A, Demitri C, Madaghiele M (2009) Biodegradable cellulose based hydrogels: Design and applications. Materials 2: 353-373.

22. Zhang S, Li FX, Yu JY (2009) Preparation of cellulose/chitin blend bio-fibers via direct dissolution. Cellulose Chemistry and Technology 43: 393-398.

23. Trovatti E, Freire CS, Pinto PC, Almeida IF, Costa P (2012). Bacterial cellulose membranes applied in topical and transdermal delivery of lidocaine hydrochloride and ibuprofen: In vitro diffusion studies. Int J Pharm 1: 83-87.

24. Fricain JC, Granja PL, Barbosa MA, de Jéso B, Barthe N (2002) Cellulose phosphates as biomaterials. In vitro biocompatibility studies. Biomaterials 23: 971-980.

25. Chong C, Zhang L (2011) Cellulose-based hydrogels: Present status and application prospects. Carbohydrate Polymers 84: 40-53.

26. Seal BL, Otero TC, Panitch A (2001) Polymeric biomaterials for tissue and organ regeneration. Materials Science and Engineering: R: Reports 34: 147-230.

27. Saito H, Sakurai A, Sakakibara M, Saga H (2003) Preparation and properties of transparent cellulose hydrogels. Journal of Applied Polymer Science 90: 3020-3025.

28. Deoliveira W, Glasser WG (1996) Hydrogels from polysaccharides. 1. Cellulose beads for chromatographic. Journal of Applied Polymer Science 60: 63-73.

29. Tovar-Carrillo KL, Sugita S, Motohiro T, Takaomi K (2013) Fibroblast compatibility on scaffold hydrogels prepared from *Agave tequilana* weber bagasse for tissue regeneration. Journal of Industrial and Engineering Chemical Research 52: 11607-11613.

30. Walkowiak B, Kesy A, Michalec L (1997) Microplate reader a convenient tool in studies of blood coagulation. Thromb Res 87: 95-103.

31. Striegel AM (1997) Theory and applications of DMAc/LiCl in the analysis of polysaccharides. Carbohydrate Polymers 34: 267-274.

32. Lindma B, Karlstrom G, Stigsson L (2010) On the mechanism of dissolution of cellulose. Journal of Molecular Liquids 156: 76-81.

33. Kacurakova M, Capek P, Sasinkova V, Wellner N, Ebringerova A (2000) FT-IR study of plant cell wall model compounds: Pectic polysaccharides and hemicelluloses. Carbohydrate Polymers 43: 195-203.

34. Pokhnel D, Viraraghava T (2004) Treatment of pulp paper mill wastewater --a review. Sci Total Environ 333: 37-58.

35. Mequanint K, Patel A, Bezuidenhout D (2006) Synthesis, swelling behavior, and biocompatibility of novel physically cross-linked polyurethane-block-poly(glycerol methacrylate) hydrogels. Biomacromolecules 7: 883-891.

36. Sjoholm E, Gustafsson K, Eriksson B, Brown W, Colmsjo A (2000) Aggregation of cellulose in lithium chloride/N_N-dimethylacetamide. Carbohydrate Polymers 41: 153.

37. Ishii D, Tatsumi D, Matsumoto T (2008) Effect of solvent exchange on the supramolecular structure, the molecular mobility and the dissolution behavior of cellulose in LiCl/DMAc. Carbohydrate Research 343: 919-928.

38. Salem AK, Stevens R, Pearson RG, Davies MC, Tendler SJ (2002) Interactions of 3T3 fibroblasts and endothelial cells with defined pore features. J Biomed Mater Res 61: 212-217.

39. Tamada Y, Ikada Q (1993) Effect of pre-adsorbed proteins on cell adhesion to polymer surfaces. Journal of Colloid Interface Science 155: 334-339.